JOURNAL OF CATALYSIS **168,** 364–373 (1997)
ARTICLE NO. CA971684

Spectroscopic Study of Active Phase-Support Interactions on a RhO_x/CeO_2 Catalyst: Evidence for Electronic Interactions

Arturo Martínez-Arias, Javier Soria, and José C. Conesa[1]

Instituto de Catálisis y Petroleoquímica, C.S.I.C., Campus Universitario de Cantoblanco, 28049 Madrid, Spain

Received July 23, 1996; revised November 18, 1996; accepted February 21, 1997

The effects of thermal treatments under vacuum, used as a way to generate reduced centers on Rh_2O_3 and RhO_x/CeO_2, have been studied by ESR and FTIR, using respectively oxygen and carbon monoxide as probe molecules. The results obtained for the outgassed samples reveal the presence of ceria–rhodia interactions favoring the stabilization of paramagnetic Rh^{2+} cations in rhodium oxide clusters on the ceria surface. Subsequent O_2 adsorption leads to the formation of different oxygen-related paramagnetic species located on ceria, on rhodium oxide clusters and at the boundary between both oxides; their contribution to the spectra depends on outgassing conditions and O_2 adsorption temperature. The unexpected absence of $O_2^- – Ce^{4+}$ species after O_2 contact at 77 K with RhO_x/CeO_2 outgassed above 573 K evidences the existence of electronic interactions between the RhO_x and CeO_2 phases, being explained on the basis of electron transfer to the mixed valence RhO_x phase from the surface-reduced ceria, leading to electron depletion of the latter. This effect is inhibited by CO adsorption, showing the dependence between the electron-accepting properties of the rhodia clusters and the presence of vacant coordination sites at the surface Rh ions. An effect of similar kind may be responsible for shifts observed in the IR bands of rhodium dicarbonyls formed in the RhO_x/CeO_2 system. The latter results suggest the possibility that thermal enhancement of surface reactions in complex systems could depend on electron transfer between adjacent phases and that adsorption on one phase may influence the surface reactivity of another phase by affecting to the electron transfer between them.

INTRODUCTION

CeO_2 is a common component of the three-way catalysts used for the elimination of toxic substances in automobile exhausts (1). Its promoting effect is thought to have both structural and bifunctional character. On the one hand, it enhances the metal dispersion (2) and stabilizes the γ-Al_2O_3 support (3); on the other hand, it works as an oxygen store (4), releasing oxygen in the presence of reductive gases and removing it in oxidizing conditions, and it may participate also in the WGS reaction (5) or in the decomposition of NO_x (6).

Several models explain these effects attributing an important role to oxygen vacancies appearing at the ceria component or at metal–ceria interfaces present in the catalysts (7, 8). The formation of such vacancies in CeO_2 and/or a supported metal oxide may modify their electrical properties and influence the interactions between both phases. Thus, metal–support electronic interactions have been proposed to explain the decrease of the energy needed for the generation of oxygen vacancies in CeO_2/Pt systems (8), which is revealed by the apparent promotion of CO oxidation with increasing ceria coverage. Earlier results on superoxide–CO interactions in $M/CeO_2/Al_2O_3$ systems (9) were similarly explained in terms of metal–semiconductor contact formation and electronic transfer between both components.

In previous work (10) we studied in detail, using ESR-monitored O_2 adsorption, the formation of anion vacancies on ceria upon outgassing. The observed ESR parameters, and the dependence of the spectra on the temperature, T_v, of the previous vacuum treatment, allowed to follow the modifications of the surface and to classify the vacancies in two main groups, isolated and associated vacancies, having different reactivity (6). In the present study the same method is used to clarify how the mutual Rh–CeO_2 interaction influences the effects of outgassing treatments on RhO_x/CeO_2 samples.

METHODS

RhO_x/CeO_2 (3 wt% Rh) was prepared by incipient wetness impregnation of CeO_2 powder (Rhône–Poulenc, $S_{BET} = 109\ m^2g^{-1}$) with aqueous rhodium nitrate. The sample was dried at 393 K for 24 h and calcined under dry air flow increasing the temperature from 295 to 673 K at 4 K min^{-1}, keeping the sample at 673 K for 4 h and cooling down to 295 K in the same flow; it was then reduced at 473 K under flowing H_2 and calcined again at 673 K. The sample thus prepared showed a surface area $S_{BET} = 93\ m^2g^{-1}$, and displayed in X-ray diffraction no other lines than those of CeO_2. Pure Rh_2O_3 ($S_{BET} = 16\ m^2g^{-1}$) was kindly provided by Johnson Matthey. Commercial gases of research purity

[1] E-mail: jcconesa@icp.csic.es.

0021-9517/97 $25.00

grade were used, being further purified by vacuum distillation methods prior to use. Vacuum and adsorption treatments were done in a conventional high vacuum line. Unless otherwise stated, doses of 70 μmol O_2/gram of catalyst were used in the ESR-oriented O_2 adsorption experiments; after each adsorption, excess O_2 was outgassed at 77 K for 15 min before taking the ESR spectra.

ESR spectra were recorded (at 77 K, unless otherwise stated) with a Bruker ER 200D system working in the X-band and calibrated with a DPPH standard ($g = 2.0036$). A special quartz probe cell provided with greaseless stopcocks was used for thermal and gas adsorption treatments. Quantitation of paramagnetic species was carried out by double integration of the ESR signals and comparison with a copper sulfate standard. A variable temperature unit was used in some cases to control the measurement temperature (T_m) in the 90–400 K range.

FTIR spectra were recorded at room temperature with a Nicolet 5ZDX spectrometer, at a resolution of 4 cm^{-1} and accumulating 100 scans for every spectrum. Thin self-supporting discs (ca 10 mg cm^{-2}) were prepared and introduced in a special glass cell described elsewhere (11), where they could be subjected to thermal or adsorption treatments.

RESULTS AND ASSIGNMENT OF SPECTRUM BANDS

ESR Spectra after Outgassing Treatments

1. Rh_2O_3. The ESR spectra of pure Rh_2O_3 outgassed at mild temperatures ($T_v \leq 473$ K) show a small, broad signal R1, with extrema at $g \approx 2.29$ and 1.99. It is already present in the initial sample (outgassed at 295 K) and increases moderately by outgassing up to $T_v = 473$ K, Fig. 1a. For $T_v \geq 573$ K, Fig. 1c, another signal R2, superimposed on signal R1, was visible mostly through an upwards broad feature at $g \approx 2.48$–2.52, the corresponding downwards feature lying probably around $g = 1.98$. At the highest signal intensity, obtained for $T_v = 573$ K, the spectrum indicates an amount of spins of ca 4 μmol/g, i.e., ca 0.05% of the total number of Rh ions. Further increase in T_v causes only a gradual decrease in these ESR lines. These signals, broad and with g values departing strongly from the free electron value $g_e = 2.0023$, must be ascribed here to Rh^{2+} ions (12–14), probably associated with defects, formed upon O_2 desorption and consequent partial reduction of Rh^{3+} cations.

2. RhO_x/CeO_2. The influence of vacuum treatments at $T_v = 373$–773 K on the ESR signals in this sample has been discussed previously (12, 13). Two main signals, also assignable to Rh^{2+}, can be observed. Signal R3, with extrema at $g = 2.26$ and 2.09 and appearing in the whole T_v range covered, is most clearly apparent after outgassing at 473 K, Fig. 2a. Signal R4, with extrema at $g \approx 2.42$ and 2.10, is seen for $T_v \geq 573$ K, its intensity increasing for higher T_v while that of signal R3 decreases. The overall intensity

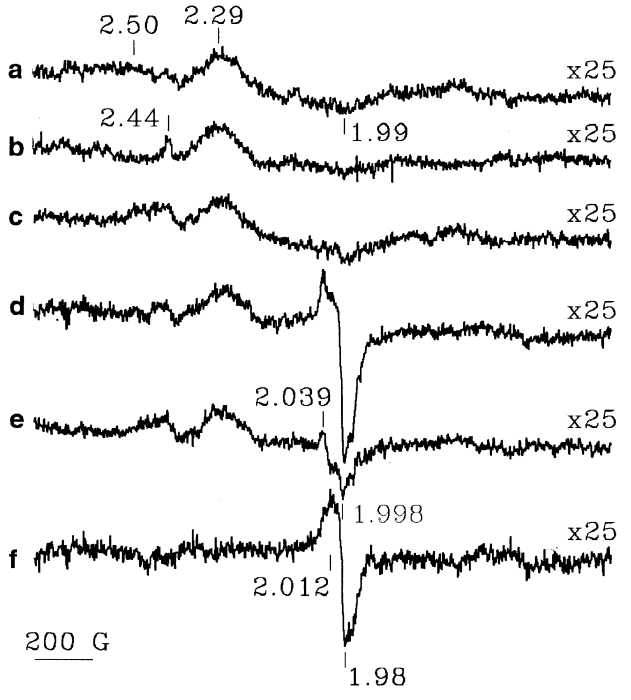

FIG. 1. ESR spectra at 77 K of Rh_2O_3: outgassed at 473 K (a), subsequently contacted with O_2 at 295 K (b), outgassed at 573 K (c), contacted again with O_2 at 295 K (d); then outgassed a 295 K (e); the difference spectrum (d)–(e) is given in (f).

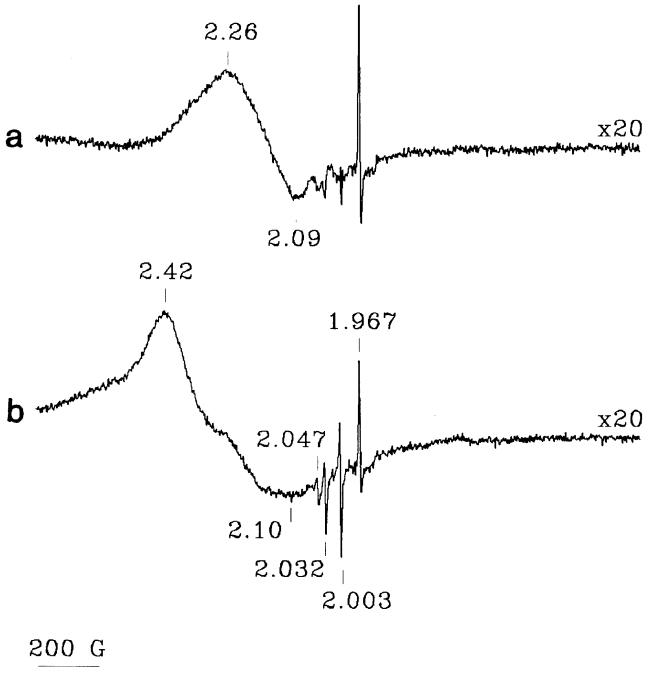

FIG. 2. ESR spectra at 77 K of RhO_x/CeO_2: outgassed at 473 K (a) and 773 K (b).

of these signals steadily increases with T_v. The highest intensity, obtained for $T_v = 773$ K, Fig. 2b, corresponds to 11 μmol/g, i.e., 3.5% of the total rhodium content. For lower outgassing temperatures such as $T_v = 373$ and 573 K, the intensities are respectively ca 10 and 2 times lower. As in the case of Rh_2O_3, these signals can be assigned to Rh^{2+} ions; their rather broad shape indicates the existence of magnetic interactions between nearby Rh^{2+} ions, which suggests that Rh_2O_3-like aggregates rather than isolated Rh ions are present at the specimen surface.

In some spectra, other small signals related to ceria were detected, showing narrow linewidths and g values not too far from g_e (between $g = 2.05$ and 1.96). They have low intensities and show small variations upon O_2 adsorption, being recovered by outgassing; they do not seem thus to be involved in any of the surface processes examined in this work.

ESR Spectra after Oxygen Adsorption

Several paramagnetic species were detected upon adsorption of O_2 on the samples studied, some of which are similar to those found for pure CeO_2 (10). The ESR parameters and characteristics of all these O_2-derived species are collected in Table 1.

1. Rh_2O_3. O_2 adsorption at $T_a \leq 295$ K on Rh_2O_3 outgassed at $T_v \leq 473$ K does not generate any new signal, Fig. 1b. For $T_v \geq 573$ K, O_2 adsorption at 77 K leads only to the elimination of the signal R2 feature $g = 2.52$. Upon subsequent warming at 295 K, the spectrum displays new features in the neighborhood of $g = g_e$, Fig. 1d, with a net increase in the overall integrated intensity. Most of the newly formed species vanish after outgassing at room temperature, leaving only a residual signal, called RO, with sharp peaks at $g = 2.039$ and 1.998, Fig. 1e. Computer subtraction (Fig. 1f) allows us to ascertain the shape of the signal eliminated through outgassing; this signal RO′ is asymmetric but with unresolved components, its upward and downward features appearing at positions $g = 2.012$ and $g = 1.98$.

Signal RO′ has overall shape and g values close to those previously observed by Shubin *et al.* (14) after O_2 adsorption on Rh/SiO_2. In agreement with those works, we assign it to a $[Rh{-}OO]^{2+}$ complex, with a two-electron σ bond between Rh^{2+} and O_2 and one unpaired electron delocalized mainly on the O–O fragment (14), Signal RO, sharper and much less intense, has a low-field g value (2.039) closer to those typical for O_2^- coordinated to trivalent ions (15). It can be ascribed also to a $[Rh{-}O_2]^{2+}$ complex, similar to that giving signal RO′, but with lower covalent mixing between the orbitals in the O_2^- fragment and those in the Rh ion, so that it can be adequately described as $[Rh^{3+}{-}O_2^-]$. The $Rh{-}O_2$ adsorption bond is here stronger, as evidenced by the permanence of signal RO after outgassing.

2. RhO_x/CeO_2. For a sample outgassed at 295 K no oxygen-derived radical appears upon contact with O_2. On the sample outgassed at $T_v = 373$ K O_2 adsorption at 77 K did not affect signal R3, but produced a new weak signal

TABLE 1

Characteristics of the ESR Signals due to Adsorbed Oxygen Species Observed in This Work and in the Previous One on CeO_2

Sample	Signal	g_z	g_y	g_x[b]	Assignment
CeO_2[a]	OI	2.037/2.035	2.011	2.011	$O_2^-{-}Ce^{4+}$ at isolated oxygen vacancies in CeO_{2-x}
	OI′	2.031	2.011	2.016	$O_2^-{-}Ce^{4+}$ at isolated oxygen vacancies in CeO_{2-x}
	OII	2.038	2.010	2.008	O_2^- at associated oxygen vacancies in CeO_{2-x}
	OII′	2.052	2.008	2.006	O_2^- at associated oxygen vacancies in CeO_{2-x}
RhO_x/CeO_2	OCR	2.028	2.011	2.017	$O_2^-{-}Ce^{4+}$ at isolated oxygen vacancies near Rh cations
	OI-OII′	[c]			[c]
		g_1	g_2	g_3	
	RO″	2.19	2.00	1.98	$[\bullet Rh{-}OO]^{2+}$ adducts
Rh_2O_3	RO	Peaks at 2.039, 1.998			$[Rh^{3+}{-}O_2^-]^{2+}$
	RO′	Extrema at $g = 2.012$, 1.98			$[Rh{-}OO\bullet]^{2+}$ adducts

[a] Values from Ref. (10).

[b] Labeling of the g values for the $O_2^-{-}Ce^{4+}$ species is chosen according to the conventions of previous works (10, 22), which assign the z axis to the highest g value and the x axis to the component displaying the highest hyperfine splitting when ^{17}O-labeled oxygen is used.

[c] These signals, first characterized on CeO_2 (10), are here observed on RhO_x/CeO_2 as well, with quite similar peak positions (g values); they are thus ascribed to the same species.

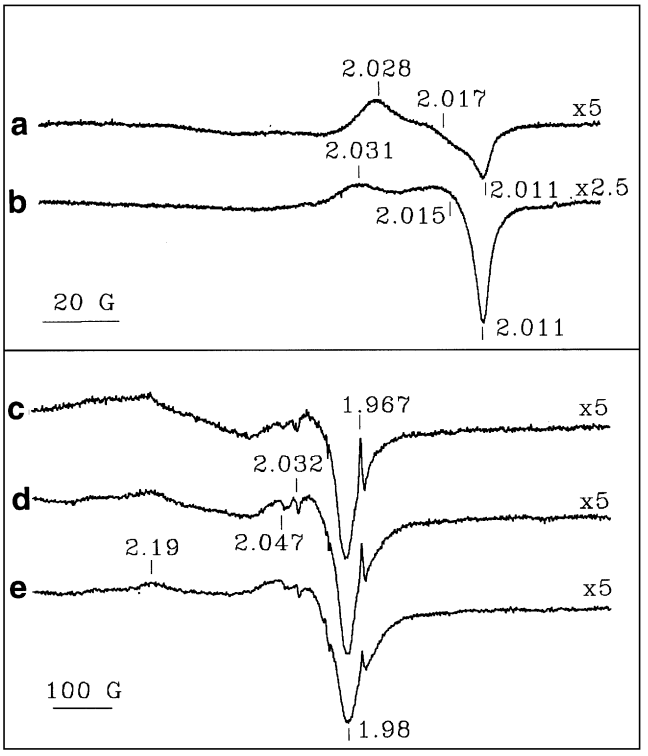

FIG. 3. ESR spectra at 77 K after O_2 adsorption at 77 K on RhO_x/CeO_2 outgassed at 373 K (a), 473 K (b), 573 K (c), 673 K (d), and 773 K (e). Note the difference in abscissa scale between (a, b) and (c–e).

OCR, with orthorhombic lineshape ($g_z = 2.028$, $g_x = 2.017$, and $g_y = 2.011$), Fig. 3a. It does not change upon warming to 295 K, except for a small lineshape modification around $g \approx 2.015$. Previous work (10) showed that, on CeO_2 outgassed at $T_v = 373$ K, no new signal was produced by O_2 adsorption at 77 K; when the adsorption temperature was increased to 295 K a signal called OI (Table 1) did appear; it was assigned to O_2^- species stabilized on Ce^{4+} ions adjacent to isolated anion vacancy sites generated by mild outgassing. Signal OCR, with ESR parameters in the same range, may be ascribed to a similar O_2^-–Ce^{4+} species, but its easier formation on a sample outgassed at 373 K (already upon adsorption at 77 K) and the noticeable difference in its ESR parameters in comparison to the CeO_2 case (10) indicate a modification of the Ce^{4+} coordination which should be due to the proximity of rhodium cations. A more marked effect of neighboring cations on O_2^-–Ce^{4+} species has recently been observed for CeO_2/Al_2O_3 (16).

For $T_v = 473$ K, O_2 adsorption at 77 K led to a decrease in signal R3 and to an O-type signal with parameters $g_z = 2.031$, $g_x = 2.015$, and $g_y = 2.011$, Fig. 3b. The latter is coincident with signal OI′, already observed for CeO_2 in similar conditions (10); it is transformed into an axial signal OI with $g_z = 2.035$, $g_x = g_y = 2.011$ upon warming at 295 K, as for CeO_2, but appears with significantly lower intensity on RhO_x/CeO_2 than on CeO_2.

For higher T_v, the results of O_2 adsorption at 77 K differ clearly from those observed on CeO_2. While in the latter case an increase of signals due to O_2^-–Ce^{4+} species, with the appearance of new signals of this kind (called OII and OII′), was observed (10), for RhO_x/CeO_2 outgassed at 573–773 K no O-type signals are produced (Figs. 3c–e), but a new broad signal RO″ appears with main peaks located around $g = 2.19$ and 1.98; it is adequately simulated with parameters $g_1 = 2.190$, $g_2 = 2.00$, and $g_3 = 1.982$. Its intensity increased with T_v and its generation is accompanied by a decrease in signals R3 and R4.

The high g_1 value of signals RO″ points to a Rh^{2+}-type species. On the other hand, its elimination upon outgassing at 295 K, the conditions for its formation and the vicinity of its g_2 and g_3 values to those corresponding to signal RO′, indicates that it contains adsorbed oxygen; it can be therefore assigned to a $[RhOO]^{2+}$ complex similar to that proposed for Rh_2O_3. The higher g_1 value, and comparison with similar species observed on other rhodium-supported samples (14, 17, 18), Table 2, indicates a substantial sensitivity of the characteristics of these complexes to the nature of the underlying support. In this case, the larger deviation of the highest g value from g_e points to the involvement of rhodium d orbitals in the semi-occupied molecular orbital, so that more unpaired electron density would remain on the Rh ion here than in the species responsible for signal RO′.

TABLE 2

Paramagnetic Rhodium–Oxygen Complexes Generated upon Oxygen Adsorption at Room Temperature on Different Supported Rhodium Samples

Sample	g tensor components	vac[a]	Assignment by authors	Ref.
Rh-A zeolite	$g_\parallel = 2.018$ $g_\perp = 1.949$	–	Rh(II)-oxygen adduct	17a
	$g_\parallel = 2.018$ $g_\perp = 1.964$	–	Rh(II)-oxygen adduct	17a
	$g_z = 2.120$ $g_x = 2.0$ $g_y = 1.954$	+	Rh(III)–O_2^-	17a
Rh-Y zeolite	$g_\parallel = 2.015$ $g_\perp = 1.931$	–	Rh(II)–O_2^{2-}–Rh(II)	17b
	$g_\parallel = 2.015$ $g_\perp = 1.944$	–	Rh(II)-oxygen adduct[b]	18
Rh-X zeolite	$g_\perp = 2.017$ $g_\parallel \approx 1.960$	–	Rh(II)-oxygen adduct[b]	17c
	$g_\parallel \approx 2.010$ $g_\perp = 1.954$	–	O_2^- covalently bound[c]	17c
	$g_z = 2.128$ $g_x = 2.014$ $g_y = 1.966$	+	Rh(II) or strongly bound oxygen	17c
Rh/silica	$g_{av} = 1.997$	–	Rh(II)–O_2 σ complex	14
Rh/Al_2O_3	$g_{av} = 2.014$	pr	Rh(II)-oxygen adduct	17d
$RhCl_3$/ $SrTiO_3$	$g_1 = 2.09$ $g_2 = 2.01$ $g_3 = 1.98$	nd	Rh(III)–O_2^-	17e
	$g_\parallel = 2.017$ $g_\perp = 1.99$	nd	Rh(II)-oxygen adduct	17e
RhO_x/CeO_2	$g_1 = 2.19$ $g_2 = 2.00$ $g_3 = 1.98$	–	Rh(II)-oxygen adduct	This work

[a] Behaviour towards outgassing at room temperature: + = stable; – = unstable; pr = partially removed; nd = not described.

[b] A structure similar to that proposed in (17b) for a similar complex, with oxygen bridging two rhodium ions, is proposed.

[c] Rhodium adsorption site not specified.

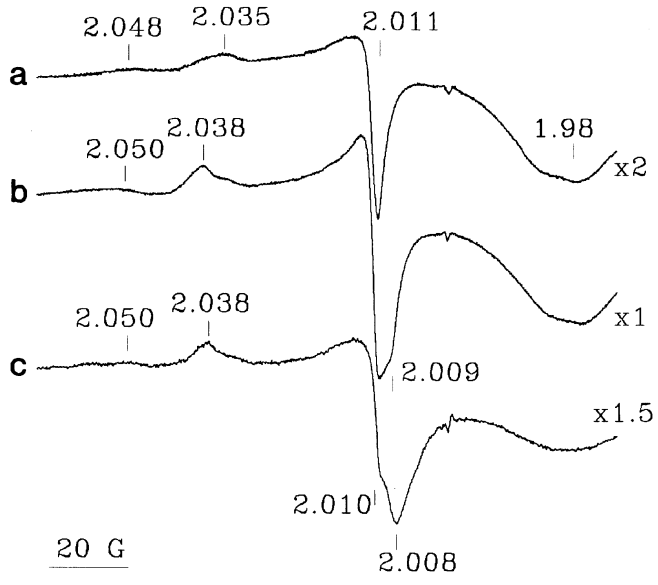

FIG. 4. ESR spectra at 77 K, after O_2 adsorption at 77 K and subsequent warming at 295 K, of RhO_x/CeO_2 previously outgassed at 573 K (a), 673 K (b), and 773 K (c).

When the sample contacted with O_2 at 77 K after outgassing at $T_v = 573$–773 K (giving the spectra in Figs. 3c–e) is warmed at 295 K, the ESR spectrum (measured again at 77 K) displays O_2^- signals, characterized by peaks in the ranges 2.038–2.050 (weak) and 2.008–2.011 (strong), Figs. 4a–c, similar to those observed upon O_2 adsorption at 77 K on similarly outgassed CeO_2 (signals OI, OII, and OII′) (10). These were assigned to O_2^- stabilized on Ce ions adjacent to oxygen vacancies, either isolated or associated (10, 19). To verify if the absence of O-type signals upon adsorption at 77 K on RhO_x/CeO_2 could be due to a too high or too low amount of O_2 added, higher amounts of this gas (350 μmol/g) were contacted in one experiment (for the case $T_v = 773$ K). This also failed to form these signals at 77 K, but led to their detection upon warming at 295 K (here with larger linewidths, evidencing magnetic dipolar broadening of the lines by the excess O_2).

This temperature-dependent O_2 adsorption was examined by obtaining ESR spectra at variable temperature, Fig. 5. Upon O_2 adsorption at 77 K on a sample outgassed at 773 K signal RO″ is observed, characterized by its component at $g = 1.98$ (only the high field part of the signal is displayed). As the measurement temperature, T_m, is raised, an initial increase in signal RO″ is produced, suggesting that its formation is a thermally activated process. Above ca 130 K its amplitude begins to decrease (which may be due to desorption, if the species is weakly held, or to mobility effects producing line broadening), while for $T_m \geq 185$ K a shoulder at $g \approx 2.008$ grows indicating the formation of O_2^-–Ce^{4+} radicals. After warming the sample to 295 K, the spectrum subsequently recorded at 77 K, Fig. 6k, displays signals RO″, with larger intensity than before warming at 295 K and type-O signals. Outgassing at 295 K produces the disappearance of signal RO″ (in the 77 K spectrum) while, in contrast with the behavior shown by pure CeO_2 (10), type-O signals are affected, their intensity being lowered. Readsorption of O_2 at 295 K produces a recovery of the signals, thus showing the reversibility of this process.

Effects of CO Adsorption

When 350 μmol/g of CO are adsorbed at 77 K on RhO_x/CeO_2 outgassed at $T_v \geq 473$ K, a well-resolved axial signal appears at $g_\perp = 2.146$ and $g_\parallel = 1.996$, Fig. 6a; this is ascribed to the formation of Rh^{2+}–CO surface complexes upon interaction of CO with exposed Rh^{2+}, which is probably a first step for the reduction of these Rh ions at 295 K (13). O_2 was subsequently added at 77 K; the Rh^{2+}–CO adduct signal then vanishes (Fig. 6b), while a type OI signal is formed, No RO″ or similar species were detected in this case.

FTIR spectra in the carbonyl stretching region, obtained for RhO_x/CeO_2 outgassed at $T_v = 473$–773 K and subsequently contacted with CO at 295 K, are given in Fig. 7. For $T_v = 473$ K, Fig. 7a, the spectrum shows mainly two

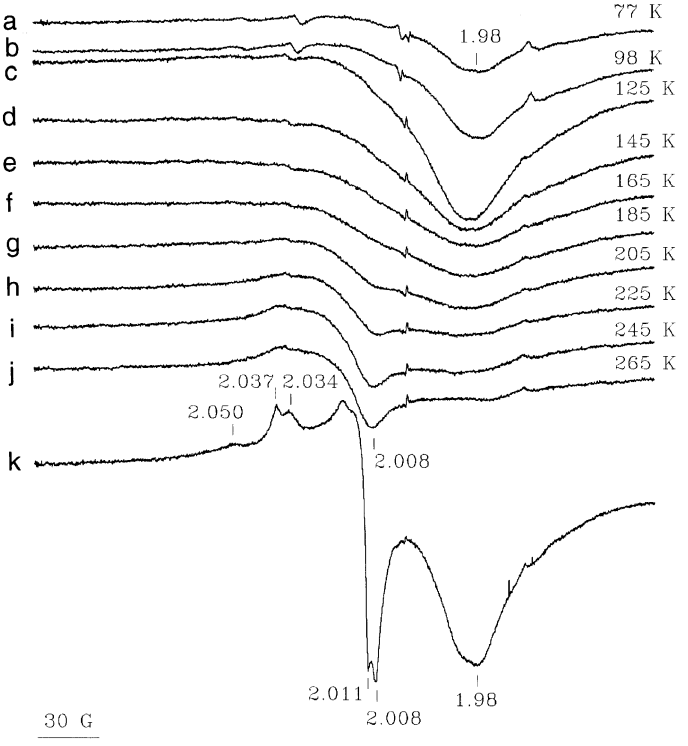

FIG. 5. ESR spectra of RhO_x/CeO_2, after outgassing at 773 K and O_2 adsorption at 77 K, recorded during gradual warming of the sample at measuring temperature $T_m = 77$ K (a), 98 K (b), 125 K (c), 145 K (d), 165 K (e), 185 K (f), 205 K (g), 225 K (h), 245 K (i), and 265 K (j), and again recorded at $T_m = 77$ K after warming at 295 K (k).

bands at 2076 and 2008 cm^{-1} ascribable to gem-dicarbonyl species (20), as confirmed by independent experiments of isotopic exchange with ^{13}CO (21). For $T_v = 573$ K, Fig. 7b, a similar spectrum is obtained; due to a larger width of these bands, some contribution of linear Rh^0 monocarbonyls (20) cannot be discarded in this case. For $T_v =$ 773 K, Fig. 7c, the higher wavenumber dicarbonyl band is shifted to 2068 cm^{-1} and has an apparently larger relative intensity. Another small and broad band appears around 1850 cm^{-1}, being assignable to bridging carbonyls formed on metallic rhodium particles (20). After additional O_2 adsorption at room temperature (the FTIR cell used does not allow to work at 77 K), Fig. 7d, the dicarbonyl bands are still observed, but they are shifted to 2087 and 2018 cm^{-1}.

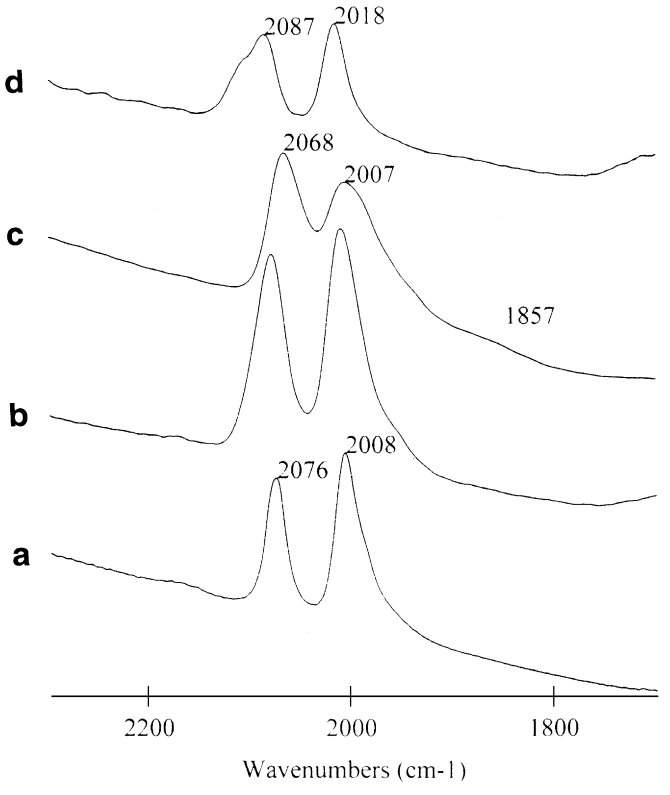

FIG. 7. FTIR spectra after adsorption of 5 Torr of CO on RhO_x/CeO_2 preoutgassed at $T_v = 473$ K (a), 573 K (b), and 773 K (c). After Fig. 7b, subsequent contact with O_2 (d).

DISCUSSION

Effect of Vacuum Treatments on Supported and Unsupported Rhodium Oxide

For Rh_2O_3, signals R1 and R2, due to Rh^{2+} ions, reveal nonstoichiometry (partial reduction), which is present to some extent already in the initial material and, as expected, increases upon outgassing due to O_2 desorption. It must be recalled that the resulting reduced Rh species may be ESR-silent if they appear as diamagnetically coupled Rh^{2+} pairs, Rh^+ ions, or Rh^0 particles, or if the electrons released become delocalized in the conduction band of the oxide. The ESR signal intensity decrease observed in this material for $T_v > 573$ K indicates an increase in these undetected states at the expense of visible Rh^{2+} ions; those states are probably Rh^{2+} pairs or Rh^+, at least for not too high T_v.

It is noteworthy that such decrease does not occur in the same T_v range for the rhodia–ceria sample. This means that the ceria support allows to stabilize reduced rhodium in the Rh^{2+} state without pairing of the excess electrons into doubly occupied orbitals. The reason for this is difficult to ascertain, since the precise structure of the Rh-containing phase in this material is not known. It may be related to the highly dispersed nature of the RhO_x surface clusters, hindering the coupling of Rh^{2+} ions in pairs, and/or due to an effect of the strongly ionic nature of the ceria surface to stabilize ions with higher charge better than Rh^+ or Rh^0. As to the absolute amounts of Rh^{2+}, it is noted that for $T_v = 573$ K (giving the highest intensity for the Rh_2O_3 sample) the fraction of Rh ions detected as Rh^{2+} is ca 35 times higher in RhO_x/CeO_2 than in pure rhodia, this ratio increasing further for higher T_v. With the present data, it cannot be decided whether this higher amount of Rh^{2+} is due to specific rhodia–ceria interactions or merely results from the high dispersion of the rhodia phase.

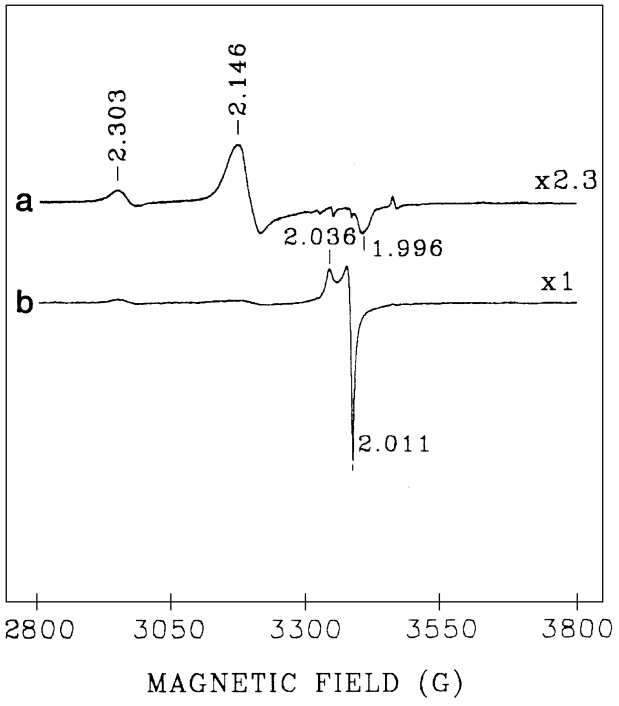

FIG. 6. ESR spectra at 77 K of RhO_x/CeO_2 outgassed at $T_v = 573$ K, after adsorption of CO (350 μmol/g) at 77 K (a), and subsequent adsorption of O_2 (70 μmol/g) at 77 K (b).

Use of Adsorbed Oxygen Species as Probe to Evidence Rhodia–Ceria Interactions

On Rh_2O_3 outgassed at $T_v \leq 473$ K, O_2 adsorption does not produce substantial changes in the spectrum. Signal R1 corresponds thus to a relatively stable center, probably associated to defects in the bulk of the oxide. Changes upon O_2 adsorption do appear when the sample has been preoutgassed at $T_v \geq 573$ K, i.e., after signal R2 is observed. The main signal formed, RO′, ascribed to a $[Rh{-}OO]^{2+}$ complex, only appears upon warming at room temperature, which indicates that the formation of this complex has here a sizeable activation energy; on the other hand, the easy elimination of this signal upon outgassing indicates a weak bonding of this complex. The other species formed by O_2 adsorption, RO, describable rather as $[Rh^{3+}{-}O_2^-]$, resists room temperature outgassing; it is therefore more stable than the $[Rh{-}OO]^{2+}$ complex, being probably formed from more reactive Rh^{2+} centers. The difference in both types of Rh^{2+} ions may reside in somewhat different environments, e.g., a different type of coordination insaturation.

$[Rh{-}OO]^{2+}$ complexes appear also on ceria-supported rhodia. As on unsupported Rh_2O_3, they appear only on samples outgassed at $T_v \geq 573$ K. Thus their formation depends on the presence of the specific type of Rh^{2+} ions which is generated by outgassing at medium-high temperatures (those giving signals R2 and R4); probably, the distinctive feature of these centers is related to the type of coordination insaturation. One difference with the Rh_2O_3 case is that, in the ceria-supported material, these complexes appear already upon O_2 adsorption at 77 K, implying that the barrier for reaction is substantially lower than on pure rhodia. Indeed, a comparison of the signal RO″ characteristics with those of other $[RhOO]^{2+}$ signals obtained on several supported rhodium systems described in the literature (Table 2) indicates that dispersion of the rhodia phase on ceria affects significantly the Rh–oxygen interaction. In our case, although the ESR parameters of signal RO″ are close to those of relatively strongly bound Rh–oxygen complexes and indicate a high spin density delocalization onto the Rh ion, the Rh–O bond remains rather weak, as in other Rh–oxygen complexes reported in the literature having g values closer to g_e.

The formation of O-type signals, due to O_2^- radicals adsorbed on Ce ions, requires the presence at the surface of excess electrons, to be transferred to the O_2 molecules, and of vacancies in the coordination sphere of the cerium ions, where the resulting O_2^- radicals may be chemisorbed. A comparison of the formation of these centers on pure ceria, discussed in detail in (10), with the results presented here for rhodia–ceria reveals significant differences, showing an influence of rhodium on the formation and properties of these oxygen vacancies.

One indication comes from the fact that the first O-type signal found on RhO_x/CeO_2, called OCR, is seen under conditions ($T_v = 373$ K, $T_a = 77$ K) for which no O_2-derived signal appeared on the support. This means that these adsorbing centers are more reactive to O_2 than those formed under the same conditions in the absence of rhodium. On the other hand, the ESR parameters of this signal are somewhat different (larger g_x and smaller g_z) from those of the similar signals (type O) found in pure ceria (Table 1), indicating a modified coordination environment of the Ce ion stabilizing the radical, an effect which should be related to the vicinity of the rhodia phase. Even though a thorough theoretical investigation about O_2^-–Ce complexes has not yet been reported, there is agreement (10, 19, 22, 23) that these deviations of g_x from g_e (the value predicted by the ionic model for adsorbed superoxide radicals (15, 24)), which are characteristic of O_2^- stabilized on Ce ions, are due to a contribution of cerium $4f$ orbitals to the superoxide–cerium bond, i.e., to covalent effects. The larger Δg_x shift observed for signal OCR suggests, thus, a modification in the bonding properties of the Ce ions at those vacancy sites which are formed at the lowest outgassing temperatures and experience the influence of nearby rhodium ions. In summary, it seems that low temperature outgassing eliminates oxygen ions at the rhodia–ceria interface (possibly from Rh–O–Ce bridges) so as to produce vacancies which are more reactive than those which appear upon the same treatment on pure ceria.

For RhO_x/CeO_2 outgassed at $T_v \geq 473$ K, subsequent O_2 adsorption gives O-type ESR signals with parameters quite similar to those observed in the case of CeO_2. The striking result concerns the thermal aspects of the formation of these radicals on the sample outgassed at $T_v \geq 573$ K. In this case, signal RO″ is observed, and no O-type signal appears, when O_2 adsorption is done at 77 K. This cannot be ascribed to dipolar broadening beyond detection due to excess physisorbed O_2, on the basis of the results with higher O_2 amounts and taking into account that these radicals were observed under similar conditions on CeO_2 (10). The absence of O-type signals implies that the O_2 molecules contacting the sample are chemisorbed exclusively on reduced rhodium centers and not on reduced cerium centers at the support. However, cerium adsorption centers with the appropriate vacant coordination sites do exist, since the corresponding O-type signals do appear upon warming already at around 180 K; and indeed they are stronger adsorption centers than those on rhodia, as shown by the experiments of desorption at 295 K after warming at the same temperature. Thus, it seems that the same type of surface centers able to adsorb O_2 on pure CeO_2, which also exists in the RhO_x/CeO_2 material, accepts O_2 already at 77 K on the former but not on the latter.

This different behavior can be explained assuming that the coordinatively unsaturated cerium centers present on

the support in outgassed RhO_x/CeO_2 cannot supply to O_2 molecules the electrons released during outgassing because, at low temperature, those electrons are trapped preferentially at the RhO_x phase, and are available only at the surface of the latter. Then, in these conditions in which molecular mobility is strongly quenched, any O_2^--like species formed on that surface will remain on it, giving rise to the RO″ species. This implies that both catalyst components are in good electronic contact, allowing the transfer of electrons between them, and requires an appropriate relationship between their electronic levels; specifically, the work function of the RhO_x phase present should be higher than that of reduced ceria, which is a *n*-semiconductor (9) and has its Fermi level close to the bottom of the conduction band. The work function of a nonstoichiometric and highly dispersed RhO_x phase such as it appears here is difficult to establish, but is expected to be higher than that of metallic rhodium, which amounts to 5.1 eV (25), while that of ceria lies between 4.7 and 2.5 eV depending on the reduction degree (26). Thus electron transfer from reduced ceria to the RhO_x phase is probably favored. It may be nearly complete if the RhO_x phase has a high density of states at the Fermi level; this would correspond to a nearly metallic character, a situation relatively common in nonstoichiometric transition metal oxides. On the other hand, stoichiometric Rh_2O_3, having closed electron shells (i.e., the valence band is full) and conduction bands which are expected to lie relatively high due to destabilization by a full coordination of the Rh ions with the oxide ligands, would probably have difficulty in accepting such electron transfer. When the latter transfer occurs, the surface region of ceria will be deleted from electrons; such effect is similar to that known to occur at metal-semiconductor contacts, leading to an interfacial electric field and an upward bending of the semiconductor bands in the zone close to the metal, i.e., to a Schottky barrier, as has been pointed out previously (9). In this situation, populating the electron levels at the cerium oxide phase will require an activation energy, being therefore dependent on the sample temperature.

These data show that, in the sample outgassed at $T_v \geq$ 573 K, Ce-bonded O_2^- species (evidenced through a feature at $g = 2.008$) begin to form upon warming at temperatures $\geq$185 K (Fig. 6). This might be explained in terms of an onset of molecular motions on the surface, by which O_2^- radicals would detach from the Rh ions (carrying the unpaired electron on the O–O fragment and leaving Rh^{3+} behind) and spill over to the ceria surface to become fixed on the more strongly adsorbing Ce^{4+} centers having coordination vacancies. However, that temperature is close to the temperature of desorption of molecular oxygen from a Rh(111) surface (27) or from polycrystalline Rh (28). Thus, it may also be that neutral oxygen molecules desorbing from the reduced rhodium centers migrate through the gas phase, at $T \geq 185$ K, to the reduced centers of the support, where

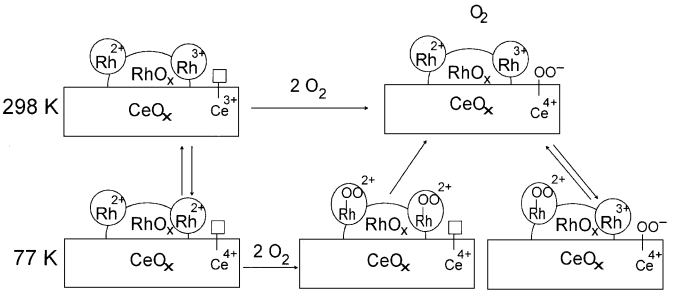

FIG. 8. Scheme of electronic states and electron transfers in the RhO_x/CeO_2 system: left side before, right side after O_2 addition; lower part at 77 K, upper part at room temperature.

they could readsorb and trap electrons if these latter, at that higher temperature, had been able to undergo thermal excitation from the levels in the RhO_x phase towards levels near the conduction band of CeO_2. Given this coincidence of onset temperatures, the second explanation seems more likely. At $T \geq 245$ K the process seems to be completed, and only a decrease in signal intensity is observed which corresponds to the expected decrease in the population difference between spin states predicted by the Boltzmann law (paramagnetic behavior). From that moment on, the system keeps $Ce–O_2^-$ species at both 77 K and 295 K, while at the latter temperature O_2 desorbs easily from the weaker $[RhOO]^{2+}$ complexes. An overall picture summarizing this model of electron transfer and localization is presented in Fig. 8.

Behavior of RhO_x/CeO_2 upon Adsorption of Other Molecules

Previous work showed (29) that both RO″ and O-type radicals could be generated on RhO_x/CeO_2 outgassed at $T_v \geq 573$ K by N_2O adsorption at 295 K (indicating a remarkable ability to form O–O bonds at such low temperature), in contrast with the behavior of pure Rh_2O_3 and CeO_2, none of which could form these species from N_2O in similar conditions. Thus, a special reactivity was evidenced for the rhodia–ceria interface in this system. On the basis of the present results, it may be proposed that the special coordination configuration of cations at that interface that allows both the easy generation of O_2^- species even at 77 K in samples outgassed at only 373 K and the stabilization without mutual coupling of substantial amounts of surface Rh^{2+} ions with high electron transfer ability, facilitates also N_2O adsorption and the transfer and further reaction of O atoms released from that molecule to form O_2 molecules. Actually, the work mentioned on N_2O reported also catalytic activity data showing that the temperature at which stoichiometric decomposition of that molecule into $N_2 + O_2$ could occur on Rh_2O_3 decreased by 50–100 K when this oxide was dispersed on ceria. This effect was ascribed to the presence of electron excess sites at microinterfaces between a partially

reduced RhO_x phase and the ceria support under reaction conditions.

The fact that, on a RhO_x/CeO_2 sample outgassed at 573 K and contacted with CO, O_2 adsorption at 77 K (Fig. 7) does not generate $[Rh{-}OO]^{2+}$ adducts, being able on the contrary to produce $O_2^-{-}Ce^{4+}$ species, may be interpreted as a result of the occupation by CO of free coordination positions on the surface Rh ions. ESR shows that the Rh^{2+} signal transforms upon CO adsorption into that of a Rh^{2+}–CO complex, so that, even if the latter is oxidized by addition of O_2 (as shown by the elimination of its ESR signal), there is no room for stabilization of a $[Rh{-}OO]^{2+}$ complex if CO is not desorbed. These results indicate anyway that, with CO adsorbed, the excess electrons are no longer trapped at 77 K on the RhO_x aggregates, but are present at the reduced CeO_2 surface, producing easily $O_2^-{-}Ce^{4+}$ species upon O_2 adsorption at that temperature. This might be due to a repulsion between the adsorbed CO and the excess electrons (or, described in another way, to a decrease in the work function of the RhO_x component upon CO adsorption), so that these electrons can return to the ceria phase. One should not exclude, however, an effect of mutual synergy between CO and O_2, already at 77 K, enhancing the oxidation of the dispersed rhodia phase (indeed, the occurrence of this phenomenon has been evidenced by XPS (30)). In any case, the possibility of modifying a surface reaction on one phase (CeO_2 here) through adsorption processes on another phase (RhO_x) via a modification of the transfer and repartition of electron between both phases is an interesting concept which might have wider applications.

The IR results obtained upon CO adsorption could be related also to electron transfer effects. The frequencies observed here for the gem-dicarbonyl rhodium complexes formed upon CO adsorption on RhO_x/CeO_2 are substantially lower than those reported for such complexes formed under similar conditions on other supports (31). In those cases, the two bands appear in the ranges 2090–2100 and 2015–2040 (here we keep the comparison within specimens prepared free from chlorine, which could affect the results). This shift indicates (32) a higher back-donation effect towards the CO fragments from the Rh^+ ions in the ceria-supported sample, suggesting a higher electron density. The blue shift of the dicarbonyl bands produced by O_2 adsorption at room temperature would indicate then the elimination of this higher electron density. It must be noted, however, that these last observations are not likely to concern to an aggregated rhodia phase, but rather to dispersed rhodium ions, as indicated by literature data (31–33) and by the absence of coverage-dependent dipolar coupling effects in these dicarbonyl bands (21). Also, this IR effect is not directly correlated to the behavior observed in ESR, as the IR shift to lower frequencies is seen already for $T_v = 473$ K. Further work is needed to verify if both observations do have the same origin.

CONCLUSIONS

The ESR data presented here show the existence, in the RhO_x/CeO_2 catalyst examined, of rhodia–ceria interactions influencing several sample properties. First, they lead to a higher stability of nonpaired, reactive Rh^{2+} ions. Second, the behavior of the O_2^- signals reveals that rhodium affects the O_2 adsorption capability of the ceria support. The reactivity of surface oxygen vacancies formed at low outgassing temperature at the ceria–rhodia boundary is higher than on pure CeO_2, due probably to a modification of the cerium coordination near the ceria–rhodia interface, while upon deeper activation electron acceptor states appear in the dispersed rhodia aggregates, leading to a depletion of electrons in the ceria support which prevents their transfer to O_2 on the surface of the latter at 77 K, the effect being suppressed by CO adsorption on the rhodia phase. It is proposed that the mentioned interfacial interaction and electronic transfer may be responsible for the enhanced catalytic activity observed for N_2O decomposition on the RhO_x/CeO_2 system (29). In any case, it is worthwhile to remark that, although the influence of electron transfer between active phase and support on catalyst reactivity is an old concept (34), the ideas that temperature may influence the surface reactivity of one of two contiguous phases mainly by changing the electron distribution between them, and, especially, that adsorption on one active phase (with CO in this case) may change the surface reactivity of another phase via a similar electron redistribution mechanism, have received little attention in the literature. They might be relevant for other situations.

ACKNOWLEDGMENTS

A.M.-A. acknowledges the Comunidad Autónoma de Madrid for a PhD grant. Financial help from CICYT (projects MAT 91-1080-CO3-O2 and 94-9835-CO3-O2) and EC (SCIENCE program, Contract SC1-CT910704) is gratefully acknowledged.

REFERENCES

1. Taylor, K. C., *Catal. Rev. Sci. Eng.* **35**, 45 (1993).
2. Dictor, R., and Roberts, S., *J. Phys. Chem*. **93**, 5846 (1989).
3. Su, E. C., and Rothschild, W. G., *J. Catal.* **99**, 506 (1986).
4. (a) Yao, H. C., and Yu Yao, Y. F., *J. Catal.* **86**, 254 (1984); (b) Engler, B., Koberstein, E., and Schubert, P., *Appl. Catal.* **48**, 71 (1989); (c) Miki, T., Ogawa, T., Haneda, M., Kakuta, N., Ueno, A., Tateishi, S., Matsuura, S., and Sato, M., *J. Phys. Chem*. **94**, 6464 (1990).
5. Shido, T., and Iwasawa, Y., *J. Catal.* **141**, 71 (1993).
6. Martínez-Arias, A., Soria, J., Conesa, J. C., Seoane, X. L., Arcoya, A., and Cataluña, R., *J. Chem. Soc. Faraday Trans.* **91**, 1679 (1995).
7. (a) Jin, T., Zhou, Y., Mains, G. J., and White, J. M., *J. Phys. Chem*. **91**, 5931 (1987); (b) Harrison, B., Diwell, A. F., and Hallett, C., *Platinum Met. Rev.* **32**, 731 (1988); (c) Leclercq, G., Dathy, C., Mabilon, C., and Leclercq, L., *Stud. Surf. Sci. Catal.* **71**, 181 (1991).
8. Hardacre, C., Ormerod, R. M., and Lambert, R. M., *J. Phys. Chem*. **98**, 10901 (1994).
9. (a) Sass, A. S., Shvets, V. A., Saveleva, G. A., Popova, N. M., and Kazanskii, V. B., *Kinet. Katal.* **27**, 894 (1986); (b) Tarasov, A. L.,

Przhevalskaya, L. K., Shvets, V. A., and Kazanskii, V. B., *Kinet. Katal.* **29**, 1181 (1988).
10. Soria, J., Martínez-Arias, A., and Conesa, J. C., *J. Chem. Soc. Faraday Trans.* **91**, 1669 (1995).
11. Fierro, J. L. G., *Stud. Surf. Sci. Catal.* **57**, B67 (1990).
12. Soria, J., Martínez-Arias, A., and Conesa, J. C., *Vacuum* **43**, 437 (1992).
13. Soria, J., Martínez-Arias, A., Fierro, J. L. G., and Conesa, J. C., *Vacuum* **46**, 1201 (1995).
14. Shubin, V. E., Shvets, V. A., and Kazanskii, V. B., *Kinet. Catal.* **19**, 1026 (1978).
15. Che, M., and Tench, A. J., *Adv. Catal.* **32**, 1 (1983).
16. Soria, J., Coronado, J. M., and Conesa, J. C., *J. Chem. Soc. Faraday Trans.* **92**, 1619 (1996).
17. (a) Goldfarb, D., Kevan, L., Davis, M. E., Saldarriaga, C., and Rossin, J. A., *J. Phys. Chem.* **91**, 6389 (1987); (b) Naccache, C., Ben Taarit, Y., and Boudart, M., *ACS Symp. Ser.* **40**, 156 (1977); (c) Goldfarb, D., and Kevan, L., *J. Phys. Chem.* **90**, 5787 (1986); (d) Yao, H. C., and Shelef, M., *in* "Proceedings of the International Congress of Catalysis, July 1980, Tokyo, Japan," paper A21; (e) Blasco, T., Conesa, J. C., and Soria, J., *Vacuum* **37**, 469 (1987).
18. Goldfarb, D., and Kevan, L., *J. Am. Chem. Soc.* **109**, 2303 (1987).
19. Zhang, X., and Klabunde, K. J., *Inorg. Chem.* **31**, 1706 (1992).
20. (a) Yates, J. T., and Kolasinski, K., *J. Chem. Phys.* **79**, 1026 (1983); (b) Yates, J. T., Duncan, T. M., Worley, S. D., and Vaughan, R. W., *J. Chem. Phys.* **70**, 1219 (1979).
21. Martínez-Arias, A., Ph.D. thesis, Universidad Autónoma de Madrid, 1994.
22. Che, M., Kibblewhite, J. F. J., Tench, A. J., Dufaux, M., and Naccache, C., *J. Chem. Soc. Faraday Trans. 1* **69**, 857 (1973).
23. (a) Védrine, J. C., Wicker, G., and Krzyzanowski, S., *Chem. Phys. Lett.* **45**, 543 (1977); (b) Mendelovici, L., Tzehoval, H., and Steinberg, M., *Appl. Surf. Sci.* **17**, 175 (1983); (c) Soria, J., Martínez-Arias, A., Conesa, J. C., Munuera, G., and González-Elipe, A. R., *Surf. Sci.* **251/252**, 990 (1991).
24. Känzig, W., and Cohen, M. H., *Phys. Rev. Lett.* **3**, 509 (1959).
25. Peebles, D. E., Peebles, H. C., and White, J. M., *Surf. Sci.* **136**, 463 (1984).
26. Pfau, A., and Schierbaum, K. D., *Surf. Sci.* **321**, 71 (1994).
27. Root, T. W., Schmidt, L. D., and Fisher, G. B., *Surf. Sci.* **134**, 30 (1983).
28. Matsushima, T., *Surf. Sci.* **157**, 297 (1985).
29. Cunningham, J., Hickey, J. N., Cataluña, R., Conesa, J. C., Soria, J., and Martínez-Arias, A., *in* "Proc. 11th Intl. Congress on Catalysis, Baltimore, 1996," *Stud. Surf. Sci. Catal.* Vol. 101, p. 681, Elsevier, Amsterdam, 1996.
30. Munuera, G., Fernández, A., and González-Elipe, A. R., *in* "Catalysis and Automotive Pollution Control II," *Stud. Surf. Sci. Catal.* **71**, Elsevier, Amsterdam, 207 (1991).
31. (a) Yao, H. C., and Rotschild, W. G., *J. Chem. Phys.* **68**, 4774 (1978); (b) Worley, S. D., Rice, C. A., Mattson, G. A., Curtis, C. W., Guin, J. A., and Tarrer, A. R., *J. Phys. Chem.* **86**, 2714 (1982); (c) *ibid.*, *J. Chem. Phys.* **76**, 20 (1982); (d) Keyes, P. K., and Watters, K. L., *J. Catal.* **110**, 96 (1988).
32. Miessner, H., Gutschick, D., Ewald, H., and Müller, H., *J. Mol. Catal.* **36**, 359 (1986).
33. Van't Blik, H. F., Van Zon, J. B. A. D., Koningsberger, D. C., and Prins, R., *J. Molec. Catal.* **25**, 379 (1984).
34. (a) Schwab, G. M., Block, J., Müller, W., and Schutze, D., *Naturwiss.* **44**, 582 (1957); (b) Szabó, Z. G., Solymosi, F., and Batta, I., *Z. Phys. Chem. N.F.* **17**, 125 (1958).